Taming the inevitable: significant parameters of teeter end impacts

V Schorbach [1], P Dalhoff [1], P Gust [2]

[1]Hamburg University of Applied Sciences, Berliner Tor 21, 20099 Hamburg, Germany
[2] University of Wuppertal, Gauss Strasse 20, 42119 Wuppertal, Germany

E-Mail: vera.schorbach@haw-hamburg.de

Abstract. Two bladed wind turbines are recently discussed more often as the question arises for the most suitable offshore turbine concept. Regarding this turbine concept, a solution for the more challenging dynamics is required. A teetered hub has been a solution for quite an amount of the former two bladed turbines. During normal operation this is an efficient possibility to eliminate the hub bending moment coming from unequal blade loading. But looking at extreme load cases the teeter end impact is a major problem. The teeter end impact is quite often described as the occasion which destroys the load reducing advantage of the teeter mechanism. However, a more detailed analysis of the intensity of the hub out of plane bending moment of the teeter end impact including influencing parameters is not given in literature. For this study, the teetered turbine CART2 from NREL is simulated with the aeroelastic tool Bladed 4.5. Design load cases leading to teeter end impacts have been identified for the CART2. The influence of different parameters of teeter end impacts will be analysed. A distinction of these parameters can be made between turbine parameters and teeter system parameters. Rotor mass and speed are turbine parameters. Pitch-teeter-coupling, the free teeter angle and the damping or stiffness of the restraint system belong to the teeter system parameters. The importance of these parameters will be investigated on three different IEC 61400-1-ed. 2 load cases leading to teeter end impacts. The simulation results will be compared with a dimensional analysis of the analytical teeter equations. Results of this study show which parameters have the most significant influence on teeter end impacts. In short, this paper will contribute to a better understanding of teeter end impacts, which are widely regarded as a severe problem but whose nature has not been the subject of a detailed analysis so far.

Nomenclature

c: blade chord
C_a: aerodynamic damping
C_h: damping constant of restraint system in hub
C_{pt}: pitch-teeter coupling coefficient
C_l: lift coefficient
$C_{l,\alpha}$: slope of lift curve
DLC: design load case
EOG: extreme operating gust
k_a: aerodynamic stiffness due to pitch teeter coupling
k_{cf}: centrifugal stiffening
k_h: stiffness of restraint system in hub
J: rotor inertia about teeter hinge
M_{EI} : end impact bending moment
r: local blade radius
R: rotor radius
u: wind speed
γ: Lock number
ζ: teeter angle
ζ_{max}: maximum teeter angle

ζ_{free}: free teeter angle
ζ_{EI}: teeter end impact range
Θ: pitch angle
Ω: rotor speed

1. Introduction

A teetered turbine is a possibility to reduce the higher dynamic loads of two bladed turbines. As long as a teetered turbine operates under normal conditions, the hub out-of-plane bending moments can be reduced significantly.
However, the additional degree of freedom of the teeter also gives the rotor the possibility to get a high amount of kinetic energy during extreme conditions. This energy must be dissipated by the teeter restraint system and may lead to high loads.
This is why teeter end impacts are often described as occasions which destroy the load reducing advantage of the teeter mechanism [1-11].
Garrad [12] defined the teeter motion as a damped forced oscillator with different parameters acting as restoring and resisting moments. Acting as a spring stiffness is the centrifugal force [k_{cf}], pitch teeter coupling [k_a] and the teeter restraint stiffness [k_h]. Aerodynamic damping [C_a] and a restraint damping of the hub [C_h] induce a resisting moment to the teeter motion.

$$J\ddot{\zeta} + (C_a + C_h)\dot{\zeta} + \left(k_{cf} + k_a + k_h\right)\zeta = M(t) \tag{1}$$

These parameters are shown in Figure 1 extended by parameters for the definition of the teeter end impact: the free teeter angle, ζ_{free}, is a range where the rotor can teeter freely without any restriction of the restraint system. The maximum teeter angle, ζ_{max}, is the teeter angle which is not allowed to be exceeded under any condition. Otherwise, the nacelle or the tower could be hit by the rotor. The teeter restraint system, consisting of a spring and/or a damper, must make sure that the maximum teeter angle will never be exceeded. The difference between ζ_{max} and ζ_{free} will be called teeter end impact range ζ_{EI}:

$$\zeta_{EI} = \zeta_{max} - \zeta_{free} \tag{2}$$

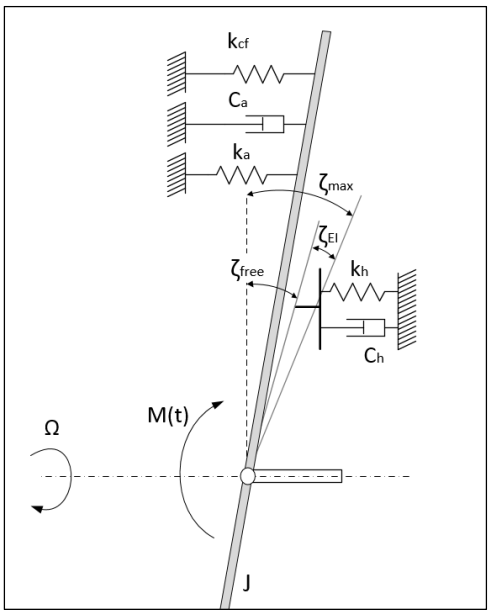

Figure 1: Principle of a teetered hub (based on [12])

The spring and damping values of equation (1) are shown in Table 1 in detail.

Table 1: Restoring and resisting moments of the teetered rotor [1, 10]

Restoring moment	description	spring / damping coefficient	requirements
M_{ka}	restoring moment of pitch-teeter coupling	$k_a = \frac{1}{2}\rho\Omega^2 C_{l\alpha}\, C_{pt} \int_{-R}^{R} c(r)\lvert r\rvert r^2 dr$	rotation, unstalled
M_{kcf}	restoring moment of centrifugal force	$k_{cf} = J\Omega^2$	rotation
M_{kh}	spring mechanical end impact in hub	design parameter of turbine depending on ζ_{EI}	free teeter angle must be exceeded; load impact on turbine
M_{Ch}	damping mechanical end impact in hub	design parameter of turbine depending on ζ_{EI}	free teeter angle must be exceeded, load impact on turbine
M_{Ca}	aerodynamic damping	$C_a = \frac{1}{2}\rho\Omega\, C_{l\alpha} \int_{-R}^{R} c(r)\lvert r\rvert r^2 dr$	rotation, unstalled

The pitch-teeter-coupling coefficient C_{pt} is the factor by which the teeter angle (ζ) leads to a pitch difference ($\Delta\Theta$).

$$\Delta\Theta = C_{pt}\zeta \tag{3}$$

A pitch-teeter coupling can be achieved by a δ_3-angle, which is a rotation of the teeter axis in the plane of rotor rotation, or by mechanical or electromechanical measures. Depending on the kind of pitch-teeter-coupling the resulting pitch-teeter-coupling coefficient according to [10] is:

$$C_{pt} = tan(\delta_3) + \frac{\Delta\Theta_m}{\zeta_m}(cos\,\delta_3)^{-1} \tag{4}$$

$C_{l\alpha}$ is the slope of the lift curve ($dC_l/d\alpha$) which is almost linear for low angles of attack.

2. Objectives

This paper intents to answer the question which design parameters of a teetered turbine have the most significant influence on the intensity of teeter end impacts. This will be done with a combination of aeroelastic simulations and a dimensional analysis of a simplified teeter end impact equation.
The turbine used for this study is the teetered CART2, operated on NREL's test site in Boulder, Colorado.

3. Approach

At first, load cases leading to teeter end impacts will be shown. Secondly, a dimensional analysis will be done with an extended teeter equation from [12]. This leads to dimensionless numbers (Chapter 3.2) which will be compared to aeroelastic simulations of teeter end impacts with changing parameters. A test plan for these simulations will be described in chapter 3.3.

3.1. Teeter end impacts of the CART2

The reference turbine for this study is the CART2. It is a 600kW teetered turbine (Westinghouse WWG600). Basic design parameters are in Table 2:

Table 2: CART2 specifications [8, 13]

CART2 specification	
Power	600kW
Rotor	diameter: 42m; hub height: 36,8m upwind; teetered
Pitch	hydraulic collective pitch
Teeter	free teeter angle: 4.5° no pitch-teeter-coupling
Teeter restraint	non-linear spring soft stop @ 4,5°: 3E06Nm/rad hard stop @ 6°: 3E07Nm/rad

The teeter restraint system of the CART2 consists of a non-linear spring. There is no teeter damper. The free teeter angle is 4.5°. Then there is a soft stop with a spring rate of 3E06 Nm/rad. When a teeter angle of 6° is exceeded a spring rate of 3E07Nm/rad defines the teeter hard stop. A hard stop is supposed to be a very unlikely event. Figure 2 shows the teeter restraint behaviour of the CART2. There is also a teeter brake on the CART2. Most teetered turbines have a teeter brake, because teeter excursions are often a problem during low rotational speed when aerodynamic damping and centrifugal forces are low [14].

For the simulations the teeter brake was deactivated in order to compare potential teeter angles during all operational stages.

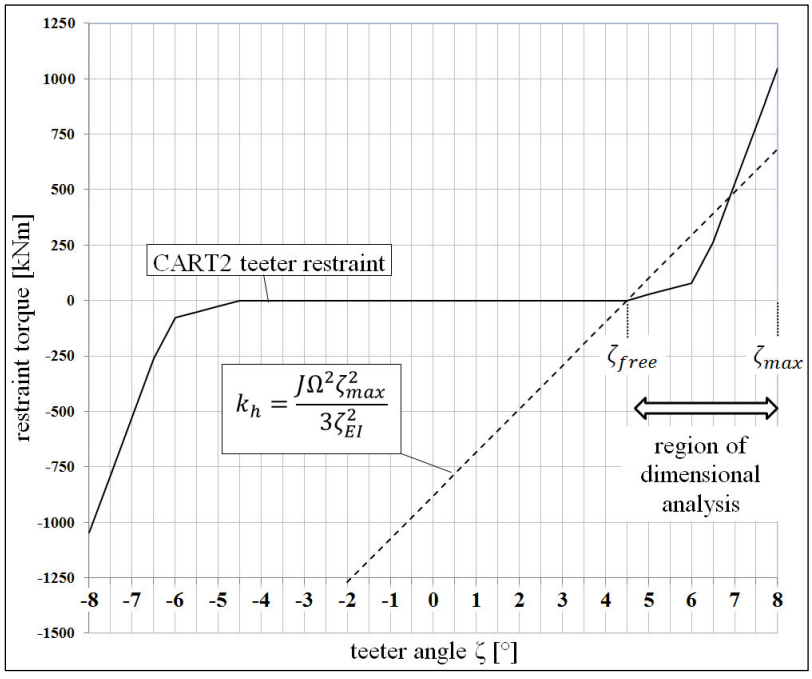

Figure 2: Teeter restraint of the CART2 (solid line), dashed line: linear simplification

Load cases leading to teeter end impacts have been identified with a load calculation of the CART2 according to IEC 61400-1 edition 2 [15]. More than 350 load cases have been simulated to find out the worst case conditions leading to teeter end impacts. All load cases leading to teeter hard stops on the CART2 baseline configuration with a non-linear teeter stiffness are in Table 5 in the appendix. For this study three severe load cases will be simulated with changing turbine parameters. As there is a significant influence of centrifugal effects and aerodynamic damping induced by rotor speed, a distinction is made between load cases during rated speed, low rotational speed and during a parked situation.
Comparing load cases with different turbine parameters is challenging concerning the turbine condition during the load case. It must be made sure that load cases happen during similar external and internal conditions. These are beside the external wind condition the same rotational speed and the same rotor azimuth. A lighter rotor mass, for example, leads to a faster start up. When comparing a startup simulation between two different rotor masses, the lighter rotor gets faster to rated speed which is a more stable condition which may prevent large teeter excursions. The load cases for this study have been chosen so that external wind conditions, rotor speed and rotor azimuth are similar for all varied turbine parameters.
These requirements lead to following three investigated load cases: A pitch fault (DLC2.1) is one of the severe load cases for teetered turbines which happen at rated rotor speed. A teeter impact happening during a reduced rotor speed is a grid loss with an extreme operating gust (DLC1.5). DLC7.1 is a parked situation with a turbine fault. This has been chosen as an extreme load cases with no rotational speed.

Table 3: Selected design load cases leading to end impacts (non-linear stiffness according to Figure 2)

DLC	Description	Rotor Speed	Teeter Angle[°]
DLC1.5	EOG and Grid Loss @25m/s + gust 14.4m/s	low rotor speed	7.7°
DLC7.1	parked and fault @ 56m/s	no rotor speed	8°
DLC2.1	Pitch fault (single blade runaway to fine) 25m/s	rated rotor speed	7.15°

3.2. Dimensional analysis of teeter end impacts

For simplification of the dimensional analysis a linear teeter stiffness has been assumed. Figure 2 shows that the potential energy between the maximum and free teeter angle of the linear stiffness is similar to the potential energy of the non-linear stiffness.
It must however be noted that a linear stiffness leads to lower maximum teeter restraint torques compared to the CART2 non-linear baseline stiffness. This effect has been obeserved in simulations with different teeter stiffnesses but it can also be seen when comparing the non-linear and linear teeter stiffness at the maximum teeter angle of 8°. The advantage of the non-linear stiffness lies in the teeter soft stop which then leads to a lower teeter restraint torque. As soft stops occur much more often than hard stops this is advantageous for turbine fatigue loads.

Having a linear teeter stiffness and a free teeter angle the equation of the teeter end impact can be written as:

$$M_{EI} = k_h(\zeta - \zeta_{free}) + C_h\dot{\zeta} = M(t) - J\ddot{\zeta} - C_a\dot{\zeta} - k_{cf}\zeta - k_a\zeta \tag{5}$$

Having such an equation a dimensional analysis can be done in order to get dimensionless numbers which may give a good information value without having the solution for the equation.
There are two principles to obtain dimensionless numbers. One is the method of Buckingham and the other one is the method of the differential equation [16, 17].

The method of the differential equation, which has been chosen for this study, has the advantage that the structure of the equation is also incorporated whereas Buckingham only regards the parameters independent of the terms of the equation.

It must be noted that this dimensional analysis is only valid for large teeter angles. Otherwise the linear simplification for k_h could not be used as it does not show a realistic behavior for small teeter angles. Figure 2 shows the valid area on the diagram with the spring stiffness of the CART2.

As the CART2 does not have a teeter damper the equation of motion is written as follows:

$$J\frac{d^2\zeta}{dt^2} + C_a\frac{d\zeta}{dt} + k_{cf}\zeta + k_h\zeta + k_a\zeta = M(t) \tag{6}$$

As only large teeter angles are considered, the subtraction of ζ_{free} from equation (5) can be omitted.
It is assumed that J, k_{cf}, k_h, C_a are independent of time.

For the dimensional analysis reference values must be defined for the time varying parameters. The purpose of the reference values is that the varying parameters will have a size of appr. 1.
As only end impacts, meaning large teeter angles, will be regarded here, all reference values will be chosen to fit into end impact situations:
For the reference value t_0 the period of one rotor turn, T, is chosen:

$$\tilde{t} = \frac{t}{t_0} \rightarrow t = \tilde{t}t_0 \qquad t_0 = T \quad \left(\Omega = \frac{2\pi}{T}\right) \tag{7}$$

The reference value of the teeter angle ζ_0 will be the maximum teeter angle:

$$\tilde{\zeta} = \frac{\zeta}{\zeta_0} \rightarrow \zeta = \tilde{\zeta}\zeta_0 \qquad \zeta_0 = \zeta_{max} \tag{8}$$

The disturbing moment coming from the wind, leading to the teeter excursion will be defined by a simple aerodynamic approach: It is assumed that the worst case situation leading to a massive teeter excursion is a high lift on one blade and zero lift on the second blade.
According to Burton, the flapwise disturbing aerodynamic teeter moment from unequal blade loading with a fluctuating wind speed component u is:

$$M(t) = \frac{1}{2}\rho\Omega c_{l\alpha}\int_{-R}^{R} u(r,t)c(r)r|r|dr \tag{9}$$

Assuming that there is lift only on one blade (the bending moment of the second blade is zero) and having a frozen wind speed fluctuation and a constant chord along the blade this can be simplified to:

$$\widetilde{M} = \frac{M}{M_0} \qquad M_0 = \frac{1}{6}\rho\Omega c_{l\alpha}cuR^3 \tag{10}$$

Putting the reference values into the equation of motion leads to:

$$J\frac{d^2\left(\tilde{\zeta}\zeta_0\right)}{d(\tilde{t}t_0)^2} + C_a\frac{d\left(\tilde{\zeta}\zeta_0\right)}{d(\tilde{t}t_0)} + \left(k_{cf} + k_h + k_a\right)\left(\tilde{\zeta}\zeta_0\right) = \widetilde{M}M_0 \tag{11}$$

This leads to five dimensionless numbers in front of the following terms:

$$\frac{d^2\tilde{\zeta}}{d\tilde{t}^2} + \underbrace{\frac{C_a t_0}{J}}_{K1}\frac{d\tilde{\zeta}}{d\tilde{t}} + \underbrace{\frac{(k_h)t_0^2}{J}}_{K2}\tilde{\zeta} + \underbrace{\frac{(k_a)t_0^2}{J}}_{K3}\tilde{\zeta} + \underbrace{\frac{(k_{cf})t_0^2}{J}}_{K4}\tilde{\zeta} = \underbrace{\frac{M_0 t_0^2}{J\zeta_0}}_{K5}\widetilde{M} \tag{12}$$

Now the reference values will be put into each dimensionless number:

$$K1 = \frac{2\pi\, C_a}{J\Omega} = \underline{\underline{\pi\rho\frac{C_{l\alpha}}{J}\int_{-R}^{R} c(r)|r|r^2 dr}} \tag{13}$$

K1 is a multiple of the Lock Number (γ), which is often used in equations of teetered rotors. The Lock Number is the ratio of aerodynamic forces to inertia forces. [14]

$$\gamma = \frac{\rho R^4 C_{l_\alpha} c}{J} \tag{14}$$

K2 is the teeter stiffness divided by the centrifugal stiffness:

$$K2 = \frac{k_h}{J\Omega^2}4\pi^2 \tag{15}$$

Now, an attempt is done to express k_h by ζ_{EI} as this is the range in which the teeter energy must be dissipated. The CART2 baseline configuration with a linear stiffness has been simulated with different end impact ranges between 1.5° and 5.5° with free teeter angles ranging from 2.5° to 6.5° and maximum teeter angle ranging from 6° to 10°. The spring stiffness was set so that the maximum teeter angle has not been exceeded during the described extreme load cases of Table 3. It has been observed that the potential energy of the teeter spring at ζ_{max} should approximately be around one third of the potential energy of the centrifugal stiffness at the ζ_{max}:

$$W_{pot,kh} = \frac{1}{2}k_h\zeta_{EI}^2 \approx \frac{1}{6}k_{cf}\zeta_{max}^2 \tag{16}$$

Results of these simulations can be seen in Table 6 in the appendix. It must be noted that this is a simple empirical approach with the help of simulation results of the CART2. Universal validity is not proven. However, it works for the regarded load cases and it offers the opportunity to express k_h by the free and maximum teeter angle. So, the teeter stiffness is now expressed as:

$$k_h = \frac{1}{3}J\Omega^2\frac{\zeta_{max}^2}{\zeta_{EI}^2} \tag{17}$$

This leads to:

$$\underline{\underline{K2 = \frac{4}{3}\pi^2\,\frac{\zeta_{max}^2}{\zeta_{EI}^2}}} \tag{18}$$

K3 is again a multiple of the Lock Number including the pitch teeter coupling coefficient:

$$K3 = \underline{\underline{4\pi^2\gamma C_{pt}}} \tag{19}$$

K4 is a constant as the centrifugal term can be cancelled down. There is no further information value:

$$K4 = \frac{(k_{cf})t_0^2}{J} = \underline{\underline{4\pi^2}} \tag{20}$$

K5 can be obtained with several steps: Using equation (10) for M_0 it can be seen that the Lock number appears again. If it is assumed that the fluctuating component is equal with the free stream velocity, u_∞, *K5* can be written with the tip speed ratio λ.

$$K5 = \frac{M_0 {t_0}^2}{J\zeta_0} = \frac{\rho\Omega c_{l\alpha} cuR^3 T^2}{6\,J\zeta_{max}} = \frac{\rho\Omega c_{l\alpha} cuR^3 4\pi^2}{6J\zeta_{max}\Omega^2} = \frac{4\pi^2}{6}\frac{\gamma}{\underline{\underline{\lambda\zeta_{max}}}} \tag{21}$$

As a next step, the information value of these dimensionless numbers will be regarded with a parameter analysis of end impacts on the CART2. This will be done with aeroelastic simulations in Bladed V4.5. According to the parameters of the dimensionless numbers, the influence of the following parameters on teeter end impacts will be analysed:

1: Lock Number (*K1*)
A change in rotor mass changes the Lock Number of the rotor. The mass of the hub and rotor will be varied to 50%, 75%, 100% and 125% of the baseline rotor mass. This leads to a variation of the Lock number between 3.5 to 9. It must however be noted that the Lock number is also part of *K3* and *K5*, which are thereby changed as well.

2: pitch-teeter-coupling (*K3*)
The influence of an aerodynamic pitch-teeter-coupling will be analysed by a variation of the δ_3-angle from 0° to 75° in steps of 15°. This makes the range for the pitch-teeter-coupling coefficient leading from 0 to 3.7.

3: free teeter angle (*K2*)
A change of the free teeter angle leads to a variation of the spring stiffness. The free teeter angle will be modified between 2.5° to 6.5°. In order to compare the results with the dimensionless numbers, the spring stiffness is assumed to be linear between the free and maximum teeter angle according to equation (17). The maximum teeter angle is set at 8°, so that *K5* is kept constant.

4: maximum teeter anlge (*K5*)
The maximum teeter angle appears in *K5* as well as in *K2*. For this study, the maximum teeter angle has been modified from 6° to 10° and the spring stiffness has been kept constant so that *K2* remains at a constant value (equation (15)). The additional variables of *K5*, tip speed ratio and Lock number, are not modified.

Table 4: Test plan for varying the end impact parameters

Test No.	parameter	range of parameter
1	free teeter angle ζ_{free}	2.5°,3.5°,4.5°,5.5, 6.5°
2	pitch-teeter-coupling by δ_3-angle	tan (0°, 15°, 30°,45°,60°,75°)
3	rotor mass (Lock Number)	50%, 75%, 100%, 125% mass of reference
4	maximum teeter angle ζ_{max}	6°,7°,8°,9°,10° (k_h=*const=1.07E07Nm/rad)*

4. Results
Figures 3 to 6 show the maximum teeter restraint torque (vertical axis) at varying teeter parameters (horizontal axis). The maximum restraint torques of the regarded load cases are shown with different colours. A second vertical axis on the right side shows the value of a dimensionless number which is modified by this parameter (factors of the dimensionless numbers consisting of a multiple of π have been left out). This is done in order to analyse, if there is a correlation between the dimensionless numbers and the magnitude of the end impact.

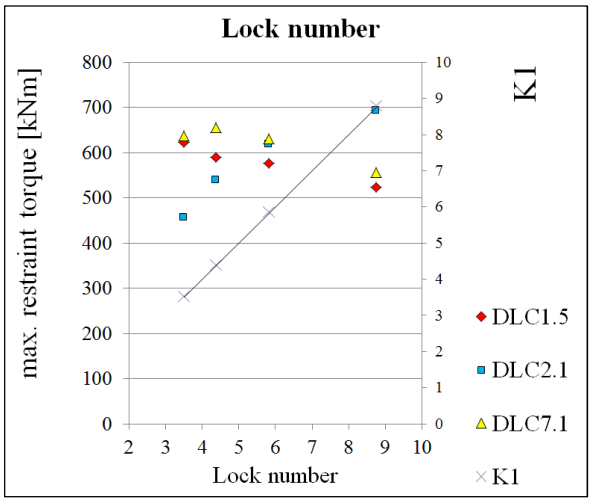

Figure 3: rotor mass (K1)

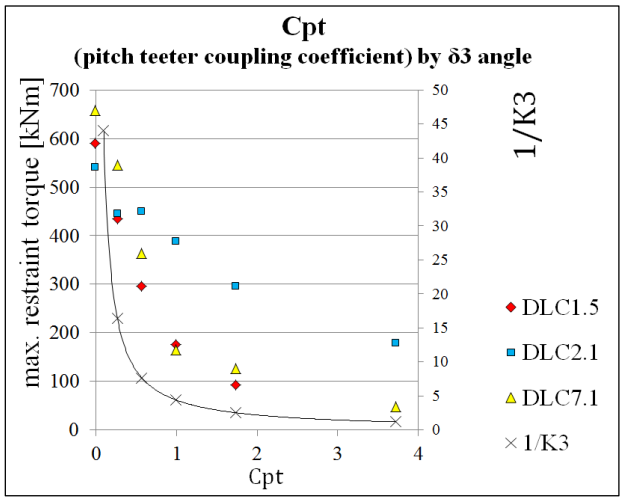

Figure 4: pitch teeter coupling coefficient (K3)

4.1. Influence of Lock Number

A change of the Lock number (Figure 3), manipulated by the rotor mass, has an almost linear influence on the end impact intensity of DLC2.1, which is an end impact occurring at full rotational speed with a massive disturbing moment coming from the pitch failure. A small Lock number, meaning that the mass of the rotor is large compared to the aerodynamic forces, leads to a larger centrifugal restoring moment and in this case to a lower end impact load. The other end impact load cases appear to become slightly lower with a rising Lock Number.

4.2. Influence of pitch-teeter-coupling

The pitch-teeter-coupling coefficient (Figure 4), modified by a δ_3-angle, has a significant effect on end impacts during low rotational speeds. The effect of DLC2.1 is lower but still existent. The behaviour comes close to the reciprocal of K3.

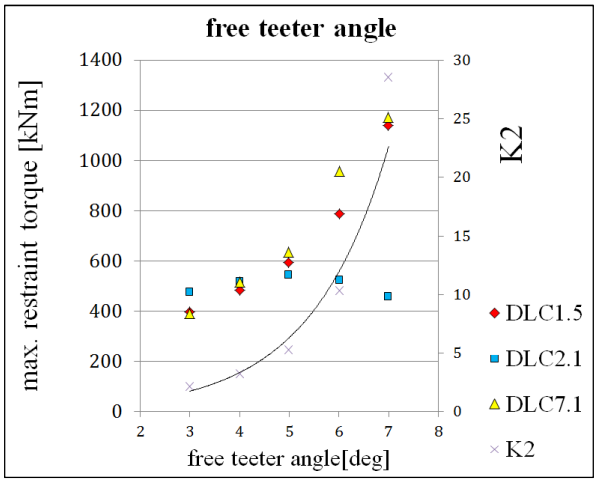

Figure 5: free teeter angle (K2)

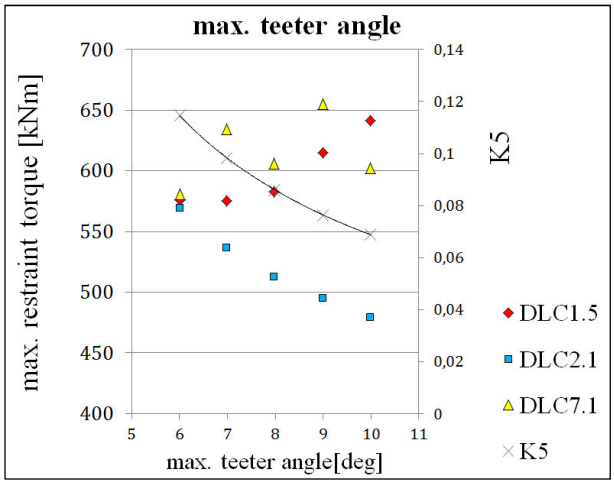

Figure 6: max. teeter angle (K5)

4.3. Influence of free teeter angle

The free teeter angle (Figure 5) has an influence on the end impact range if the max. teeter angle remains constant. It has a significant influence on the intensity of load cases with low rotational speed.

The corresponding dimensionless number is K2, which also represents the approach of the stiffness for the teeter restraint in equation (17).

4.4. Influence of maximum teeter angle

The maximum teeter angle is modified in Figure 6. The end impact intensity of DLC2.1 fits well with K5. However, the other load cases do not. There is even an increase of end impact intensity of DLC1.5 with a larger maximum teeter angle.

5. Discussion

A dimensional analysis of the teeter equation with a linear approach of the hub stiffness was used to obtain dimensionless numbers. Besides the already known Lock number, additional numbers characterising teeter end impacts have been shown. These analytic results have been compared with aeroelastic simulations of turbine conditions leading to teeter end impacts.

First, it may be noted that an analytic approach of a turbine design is a very helpful addition to aeroelastic simulations especially when modifying multiple parameters.

As three quite different load cases of the simulation have been used for the comparison against the analytic results a perfect fit of the dimensionless numbers has not been expected. The results show however that a further investigation seems to be worthwhile. The influence of the teeter parameters on the intensity of teeter end impacts is not similar for all end impact situations. A pitch fault occurring at rated rotor speed shows a different behaviour towards teeter parameters than end impacts happening at lower rotor speeds. A reduced free teeter angle appears to be useful for end impacts with lower rpms (regarding extreme loads only; a certain size of the free teeter angle is essential to reduce operational loads; this is the original idea of a teetered turbine at all). A large maximum teeter angle has a positive effect on load cases happening at rated rotor speed. Its influence is rather negative for load cases with low rotational speed. A pitch-teeter-coupling has a load mitigating effect on all end impact load cases. It has two advantages: first: it reduces teeter angles under normal operating conditions and thus allows reducing the free teeter angle. Second: the end impact intensity minimises significantly with a pitch-teeter-coupling. Although the Lock number has not been modified independently of the other dimensionless numbers, it can be observed, that a large Lock number may have a negative effect on certain load cases. This needs further study with regards to the relatively large Lock numbers of today's turbines.

An empirical approach for calculating the teeter stiffness of the CART2 with the help of the free and maximum teeter angle has been used. Further studies must show if this is a useful approach for other turbines as well. With regards to the results of the Lock number, it must be investigated if the Lock number may also be considered in this approach.

Further research is of vital importance as teeter end impacts are quite serious. However, there are controllable turbine parameters which allow a significant load reduction.

The next steps are to prove the validity of the dimensionless numbers on different turbine models and to show the most suitable combination of teeter parameters to reduce the loads of end impacts. This will be done including additional teeter end impact load cases.

With the results of the next steps it can be seen, to what extent reductions of the intensity of teeter end impacts are possible. This will be a contribution to the upcoming discussion on two bladed turbines.

6. Acknowledgements

We would like to thank DNVGL-Energy for providing a Bladed license for this research.

Additionally, we thank Peter Wulf from HAW Hamburg for valuable discussions on dimensional analysis.

Appendix

Table 5: extreme load cases according to IEC61400-1 edition 2 leading to teeter hard stops on the CART2

ranking	DLC	max. teeter angle [°]	design condition	rotor speed
1	DLC7.1	8,01	parked & fault	no rpm
2	DLC3.3	7,87	startup & extreme direction change	low rpm
3	DLC1.5	7,68	extreme operating gust (1year) + grid loss	low rpm
4	DLC6.1	7,56	parked/idling	no rpm
5	DLC5.1	7,50	emergency shut down	low rpm
6	DLC3.2	7,20	startup& extreme operating gust	low rpm
7	DLC2.1	7,15	power production + fault	rated rpm
8	DLC4.1	7,11	normal shut down	low rpm
9	DLC3.1	7,06	startup	low rpm
10	DLC1.3	6,06	extreme coherent gust with direction change	rated rpm

Table 6: simulated maximum teeter angles with a spring stiffness based on ζ_{free} *and* ζ_{max} according to equation (17)

ζ_{free} [°]	ζ_{max} [°]	simulated ζ_{max} **DLC2.1** [°]	simulated ζ_{max} **DLC7.1** [°]	simulated ζ_{max} **DLC1.5** [°]
2.50	8	8.46	7.45	7.55
3.50	8	7.87	7.86	7.59
4.50	8	7.29	7.75	7.54
5.50	8	6.87	8.00	7.56
6.50	8	6.93	7.61	7.57
3.30	6	6.37	6.43	6.40
3.90	7	6.75	7.27	6.95
4.40	8	7.17	7.67	7.55
5.00	9	7.63	8.49	8.27
5.50	10	8.09	8.76	8.96

References

[1] Burton T. Jenkins N. Sharpe D. Bossanyi E. Wind Energy Handbook: John Wiley & Sons; 2011.
[2] Jamieson P. Innovations in Wind Turbine Design. West Sussex. UK: John Wiley & Sons. Ltd; 2011.
[3] Hau E. Windkraftanlagen. Berlin: Springer; 2008.
[4] Bossanyi E. Savini B. Iribas M. Hau M. Fischer B. Schlipf D. Advanced controller research for multi-MW wind turbines in the UPWIND project. Wind Energy. 2012;15(1):119-45.

[5] Quell P. Vergleich von starrer und Pendel-Rotornabe für eine Windkraftanlage der Megawatt-Leistungsklasse am Beispiel der WKA Autoflug A 1200. DEWEK; 1996; Wilhelmshaven. Germany.
[6] Hansen AC. Yaw Dynamics of horizontal Axis Wind Turbines. National Renewable Energy Lab. 1992.
[7] Malcolm D. Response of stall-controlled. teetered. free-yaw downwind turbines. Wind Energy. 1999;2(2):79-98.
[8] Stol K. Geometry and structural properties for the controls advanced research turbine (CART) from model tuning. NREL/SR. 2003:500-32087.
[9] Hohenemser K. Analysis and test results for a two-bladed. passive cycle pitch. horizontal-axis wind turbine in free and controlled yaw. National Renewable Energy Lab.. Golden. CO (United States); Washington Univ.. St. Louis. MO (United States). 1995.
[10] Henderson G. Haines R. Quarton D. The Analysis and Design Implications of Pitch Teeter Coupling. Proc EWEC; 1989.
[11] Van Kuik G. Dekker J. The FLEXHAT program. technology development and testing of flexible rotor systems with fast passive pitch control. Journal of Wind Engineering and Industrial Aerodynamics. 1992;39(1):435-48.
[12] Garrad A. The Prediction of Teeter Excursions on a horizontal axis wind turbine. 4th BWEA Conference; Cranfield1982.
[13] personal communication. National Renewable Energy Lab 2013.
[14] Manwell JF. McGowan JG. Rogers ALU. Wind Energy Explained: Theory. Design and Application: Wiley; 2010.
[15] International Electrotechnical Commission. IEC 61400-1 second edition 1999-02 Wind turbine generator systems – Part 1: Safety requirements. 1999.
[16] Spurk JH. Dimensionsanalyse in der Strömungslehre: Springer-Verlag; 1992.
[17] Pawlowski J. Die Ähnlichkeitstheorie in der Physikalisch-Technischen Forschung: Grundlagen und Anwendung: Springer London. Limited; 2011.